Compel

Asymptotic Fourier decomposition of tooth forces in terms of convolved air gap field harmonics for noise diagnosis of electrical machines

M. van der Giet
Institute of Electrical Machines, RWTH Aachen University, Aachen, Germany
R. Rothe
Institute of Electrical Machines, RWTH Aachen University, Aachen, Germany
K. Hameyer
Institute of Electrical Machines, RWTH Aachen University, Aachen, Germany

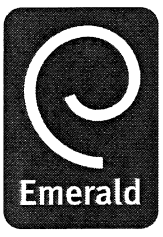

Compel, Vol. 28 No. 4, 2009,
 ISSN 0332-1649

COMPEL exists for the discussion and dissemination of computational and analytical methods in electrical and electronic engineering. The main emphasis of papers is on methods and new techniques, or the application of existing techniques in a novel way. Whilst papers with immediate application to particular engineering problems are featured, so too are papers that form a basis for further development in the area of study. A double-blind review process ensures the content's validity and relevance.

Typeset in India by the OKS Group

ISBN 978-1-84855-722-2
ISSN 0332-1649

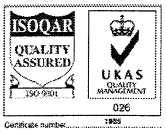

Awarded in recognition of Emerald's production department's adherence to quality systems and processes when preparing scholarly journals for print

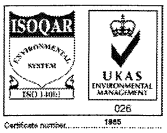

Emerald Group Publishing Limited, Howard House, Environmental Management System has been certified by ISOQAR to ISO14001:2004 standards

COMPEL is indexed and abstracted in:
Compendex Plus
Engineering Index
INSPEC®
Mathematical Reviews
Scopus
Thomson Scientific Alerting Service®
Thomson Scientific COMPUMATH Citation Index®
Thomson Scientific Current Contents®:
Engineering, Computing and Technology
Thomson Scientific SciSearch®: Science Citation Index Expanded
Zentralblatt MATH
zetoc

This journal is also available online at:
Journal information
www.emeraldinsight.com/compel.htm
Table of contents
www.emeraldinsight.com/0332-1649.htm

Online journal content available worldwide at www.emeraldinsight.com

Emerald Group Publishing Limited
Howard House, Wagon Lane,
Bingley BD16 1WA, United Kingdom
Tel +44 (0) 1274 777700
Fax +44 (0) 1274 785201
E-mail **emerald@emeraldinsight.com**

INVESTOR IN PEOPLE

Regional offices:

For Americas
Emerald Group Publishing Inc., One Mifflin Place, 119 Mount Auburn Street, Suite 400, Harvard Square, Cambridge, MA 02138, USA
Tel +1 617 576 5782
E-mail **america@emeraldinsight.com**

For Asia Pacific
Emerald, 7-2, 7th Floor, Menara KLH, Bandar Puchong Jaya, 47100 Puchong, Selangor, Malaysia
Tel +60 3 8076 6009; Fax +60 3 8076 6007
E-mail **asia@emeraldinsight.com**

For Australia
Emerald, PO Box 1441, Fitzroy North, VIC 3068, Australia
Tel/Fax +61 (0) 3 9486 2782; Mobile +61 (0) 4315 98476
E-mail **australasia@emeraldinsight.com**

For China
Emerald, 7th Xueyuan Road, Haidian District, Room 508, Hongyu Building, 100083 Beijing, People's Republic of China
Tel +86 108-230-6438
E-mail **china@emeraldinsight.com.cn**

For India
Emerald, 301, Vikas Surya Shopping Mall, Mangalam Place, Sector -3, Rohini, New Delhi - 110085, India
Tel +91 112 794 8437/8
E-mail **india@emeraldinsight.com**

For Japan
Emerald, 92-5 Makigahara, Asahi-ku, Yokohama 241-0836, Japan
Tel/Fax +81 45 367 2114
E-mail **japan@emeraldinsight.com**

For African enquiries
E-mail **africa@emeraldinsight.com**

For European enquiries
E-mail **europe@emeraldinsight.com**

For Middle Eastern enquiries
E-mail **middleeast@emeraldinsight.com**

Customer helpdesk:
Tel +44 (0) 1274 785278; Fax +44 (0) 1274 785201;
E-mail **support@emeraldinsight.com**
Web **www.emeraldinsight.com/customercharter**

Orders, subscription and missing claims enquiries:
E-mail **subscriptions@emeraldinsight.com**
Tel +44 (0) 1274 777700; Fax +44 (0) 1274 785201

Missing issue claims will be fulfilled if claimed within six months of date of despatch. Maximum of one claim per issue.

Hard copy print backsets, back volumes and back issues of volumes prior to the current and previous year can be ordered from Periodical Service Company. Tel +1 518 537 4700;
E-mail **psc@periodicals.com** For further information go to **www.periodicals.com/emerald.html**

Reprints and permission service
For reprint and permission options please see the abstract page of the specific article in question on the Emerald web site (**www.emeraldinsight.com**), and then click on the "Reprints and permissions" link. Or contact:
Copyright Clearance Center- Rightslink
Tel +1 877/622-5543 (toll free) or 978/777-9929
E-mail **customercare@copyright.com**
Web **www.copyright.com**

Emerald is a trading name of Emerald Group Publishing Limited

Printed by Printhaus Group Ltd, Scirocco Close, Moulton Park, Northampton NN3 6HE

Asymptotic Fourier decomposition of tooth forces in terms of convolved air gap field harmonics for noise diagnosis of electrical machines

M. van der Giet, R. Rothe and K. Hameyer
Institute of Electrical Machines, RWTH Aachen University, Aachen, Germany

Abstract

Purpose – The electromagnetic excited audible noise of electrical machines can be mostly attributed to radial forces on stator tooth-heads. The methodology proposed in this paper uses numerical field simulation to obtain the magnetic air gap field of electrical machines and an analytical-based post-processing approach to reveal the relationship between air gap field harmonics and the resulting force wave.

Design/methodology/approach – The simulated air gap field is sampled in space and time and a two-dimensional Fourier transform is performed. The convolution of the Fourier transformed air gap field by itself represents a multiplication in space time domain. During the convolution process, all relevant combinations of field waves are stored and displayed using space vectors.

Findings – The effectiveness of the proposed approach is shown on an example machine. Particular examples of individual force waves demonstrate how the approach can be used for practical application in analysis of noise and vibration problems in electrical machines. The proposed method is compared to the result of a Maxwell stress tensor calculation. It shows that the deviation is small enough to justify the approach for analysis purposes.

Originality/value – The combination of analytically understood force waves and the use of numerical simulation by means of air gap field convolution has not been proposed before.

Keywords Vibration, Electric machines, Noise control, Simulation, Finite element analysis

Paper type Research paper

1. Introduction

The reduction of audible noise in electrical machines is attracting more and more attention. Designing low noise electrical machines requires a good understanding of the causes of noise excitation.

Classical analytical approaches for noise analysis in electrical machines rely on the identification of space and time harmonics in the air gap field that generate radial magnetic force waves (Jordan, 1950; Gieras *et al.*, 2006). The causality relation between force waves and field harmonics can be traced back this way. The drawback of such methods, however, is the limited accuracy of the air gap field and magnetic force wave amplitudes.

Numerical simulations, with, e.g. the finite element method (FEM), are able to capture finer details and allow an accurate determination of air gap field and magnetic force amplitudes (Gieras *et al.*, 2006; Furlan *et al.*, 2003; Schlensok *et al.*, 2007). Under the standard linear assumption, the vibroacoustic problem is most commonly solved in the

COMPEL: The International Journal for Computation and Mathematics in Electrical and Electronic Engineering
Vol. 28 No. 4, 2009
pp. 804-818

0332-1649
DOI 10.1108/03321640910958937

frequency domain, either by modal analysis and superposition, or by immediate harmonic analysis. In both cases, the computed electromagnetic force excitations are transformed into the frequency domain. Besides, the Fourier transform of time waves, spatial waves are also transformed in order to identify the spatial wave numbers of the air gap field. Comparing the wave numbers and frequencies with those obtained from analytical models, it is possible to identify which magnetic field harmonic predominantly contributes to a given force wave (Kobayashi *et al.*, 1997).

However, it is not possible by this approach to find out the exact composition of each force wave. The approach presented in this paper overcomes this fundamental drawback by Fourier transforming the magnetic field in time and space directly so as to obtain a representation of the air gap field as a function of wave numbers and frequencies.

The outline of this paper reads as follows: first the analysis of magnetic force waves by means of the analytical model is explained. Afterwards a brief review of the two-dimensional discrete Fourier transform (2D DFT) and the usage of space vectors is given. The subsequent section presents numerical results for one example machine and a summary concludes the paper.

2. Generation of magnetic force waves

The air gap field in electrical machines cause force densities on the permeable material of the stator and rotor teeth. Featuring different frequency components, these forces are responsible for mechanical vibrations that radiate air-borne sound.

Magnetic forces acting on a given medium are the divergence of the electromechanical tensor of that medium. Each medium has its own electromechanical tensor, and that of empty space, or air, is the celebrated Maxwell stress tensor (MST) (Henrotte and Hameyer, 2007). In consequence, magnetic forces come under volume and surface density form. In saturable non-conducting materials, the volume density is basically related with the gradient of the magnetic reluctivity, and it is usually negligible with respect to the surface force density. The latter, located at material discontinuities (e.g. on the stator surface in the air gap), is the divergence in the sense of distribution of the electromechanical tensor. It can be shown (Melcher, 1981) that it has a normal component only, whose amplitude is:

$$P_r = \left[B_r(H_{1r} - H_{2r}) - \left(w_1' - w_2'\right)\right], \tag{1}$$

where B_r is the radial magnetic flux density at the interface between the stator and the air gap. H_{1r} and H_{2r} are the radial magnetic field strength in the air and in the stator iron, respectively. The magnetic co-energy density w' is related to the magnetic energy density w by:

$$w' = H(B)\cdot B - w(B) = H(B)\cdot B - \int_0^{|B|} |H(x)|dx. \tag{2}$$

Owing to the constant magnetic permeability of air, w_1' is:

$$w_1' = H\cdot B - \frac{1}{2}H\cdot B = \frac{|B|^2}{2\mu_0}, \tag{3}$$

where μ_0 denotes the magnetic permeability of vacuum. If the permeability of the iron cannot be considered constant, the magnetic energy term of the iron has to be determined by means of numerical integration along the BH-curve, otherwise, i.e. in the linear case, equation (1) can be simplified to:

$$P_r = \frac{1}{2}[B_r(H_{1r} - H_{2r}) - H_t(B_{1t} - B_{2t})]. \tag{4}$$

If in addition, the permeability of the iron is sufficiently large and the magnetic field strength in the iron can be neglected, the magnetic force density is finally approximated by:

$$P_r = \frac{B_r^2}{2\mu_0}. \tag{5}$$

In steady state operation, the air gap field is periodic in time and space, and it is commonly described by a Fourier series of a one-dimensional wave by Jordan (1950):

$$b(x,t) = \sum_{i=0}^{\infty} \hat{B}_i \cos(\nu_i x - \omega_i t - \Psi_i), \tag{6}$$

where ν_i is the wave number, also called "number of pole pairs", and ω_i is the corresponding frequency of one particular wave. Applying equation (5) gives the force density in the air gap:

$$\begin{aligned} p(x,t) &= \frac{1}{2\mu_0}\left[\sum_{j=1}^{\infty} \hat{B}_i \cdot \cos(\nu_j x - \omega_j t - \Psi_j)\right]^2 \\ &= \frac{1}{2\mu_0}\sum_{k=1}^{\infty}\sum_{l=1}^{\infty} \hat{B}_k\hat{B}_l \cdot \cos(\nu_k x - \omega_k t - \Psi_k)\cdot\cos(\nu_l x - \omega_l t - \Psi_l) \\ &= \frac{1}{2\mu_0}\sum_{k=1}^{\infty}\sum_{l=1}^{\infty} \frac{\hat{B}_k\hat{B}_l}{2} \cdot \cos((\nu_l \pm \nu_k)x - (\omega_l \pm \omega_k)t - \Psi_l \pm \Psi_k) \\ &= \sum_{k=1}^{\infty}\sum_{l=1}^{\infty} \hat{P}_{kl} \cdot \cos(r_{kl}x - \omega_{kl}t - \Psi_{kl}), \end{aligned} \tag{7}$$

with:

$$\hat{P}_{kl} = \frac{\hat{B}_k\hat{B}_l}{2\mu_0}, \quad r_{kl} = \nu_l \pm \nu_k, \quad \omega_{kl} = \omega_l \pm \omega_k, \tag{8}$$

Force waves combine magnetic flux density waves two by two. As the wave numbers of the force waves are strongly related with the vibrational eigenmodes of the stator, they are also called mode numbers.

One common method to analyze magnetic force density waves is Jordan's combination table (Jordan, 1950), by which the air gap field $b(x, t)$ is calculated from the

permeance function of the machine and the magnetomotive forces. As shown in Table I, the causes of typical air gap field harmonics can be derived. The wave numbers of harmonics excited by stator or rotor slotting, winding distribution or saturation are well known and described by the number of stator and rotor slot N_1 and N_2, the number of pole pairs p, the frequency of the fundamental component f_p. Simplifying assumptions and effects like saturation diminish the accuracy of quantitative statements concerning the amplitude of higher harmonics. In addition, it happens in practice that force density harmonics are obtained by finite element (FE) analysis that were not identified by the analytical model.

3. Analysis of magnetic force density waves using numerical simulation data and a convolution approach

In comparison to the analytical approach, a two-dimensional electromagnetic FEM simulation provides an accurate representation of the magnetic flux density distribution. The air gap field can be sampled in time and space and the Fourier series coefficients can subsequently be approximated by means of the DFT. Since many air gap field waves combinations have the same wave number, a magnetic force density harmonic is usually the geometrical sum of a number of pairs of air gap field harmonics. The common approach of applying Fourier analysis to the force densities does not provide information about their composition. Before discussing the presented approach, the two-dimensional DFT and the usage of space vectors is briefly reviewed.

3.1 Two-dimensional Fourier analysis

Say $T > 0$, $\omega = 2\pi/T$ and $f : [0, 2\pi] \times [0, T] \rightarrow \mathbb{C}$ is a piecewise differentiable function. Then f can be represented by a Fourier series:

$$f(x,t) = \sum_{n=-\infty}^{\infty} \sum_{m=-\infty}^{\infty} c_{nm} e^{j(nx+m\omega t)}. \tag{9}$$

The complex coefficients of the Fourier series are determined by:

$$c_{nm} = \frac{1}{2\pi T} \int_0^{2\pi} \int_0^{T} f(x,t) e^{-j(nx+m\omega t)} dt dx. \tag{10}$$

The function f now be sampled at discrete locations in space:

$$x_k = k\Delta x, \quad k \in \mathbb{Z}, \quad \Delta x > 0 \tag{11}$$

and discrete instants in time:

Cause	Wave number (ν)	Frequency order (w/w_0)
Stator slotting	$gN_1 + p,\ g \in \mathbb{N}$	1
Rotor slotting (IM)	$gN_2 + p,\ g \in \mathbb{N}$	$1 + (gN_2/p) \cdot (1 - s)$
Stator winding distribution	$p(6g + 1),\ g \in \mathbb{Z}$	1
Current harmonic (μ)	$p(6g + \mu),\ g \in \mathbb{Z}$	μ
Saturation	3p	3

Table I. Wave numbers and frequencies of typical air gap field harmonics

$$t_l = l\Delta t, \quad l \in \mathbb{Z}, \quad \Delta t > 0. \tag{12}$$

If in addition, f is periodic in space and is sampled N times ($2\pi = N\Delta x$) and if it is also periodic in time with M sample points ($T = M\Delta t$, $\omega = 2\pi/T$), then the function can be completely described by a matrix $Y \in \mathbb{C}^{N\times M}$. For the sake of simplicity $N, M \in \mathbb{N}$ be odd.

The 2D-DFT, as approximation for the Fourier series of the function is defined as unique invertible linear mapping $\text{2D-DFT} : Y \in \mathbb{C}^{N\times M} \rightarrow \bar{Y} \in \mathbb{C}^{N\times M}$ by means of the spectral coefficients:

$$\bar{y}_{nm} = \frac{1}{NM} \sum_{k=0}^{N-1} \sum_{l=0}^{M-1} y_{kl} e^{-j(nx_k + m\omega t_l)}, \tag{13}$$

where y_{kl} are entries of the matrix $Y \in \mathbb{C}^{N\times M}$ and $\bar{y}_{nm}$ are entries of the matrix $\bar{Y} \in \mathbb{C}^{N\times M}$. The inverse mapping is called the two-dimensional inverse Fourier transform (2D-IDFT) and is defined by:

$$y_{kl} = \sum_{n=0}^{N-1} \sum_{m=0}^{M-1} \bar{y}_{nm} e^{j(nx_k + m\omega t_l)}. \tag{14}$$

There are algorithms, such as the Fast Fourier Transform that efficiently compute equations (13) and (14).

The matrix Y approximates the function f, and $\bar{Y}$ its spectrum. If f is real, i.e. $y_{nm} \in \mathbb{R}\ \forall n, m$, then it can be written in the following form:

$$f(x,t) \approx \sum_{n=0}^{N-1} \sum_{m=0}^{M-1} A_{nm} \cos(r_n x + m\omega t + \varphi_{nm}), \tag{15}$$

where $r_n = n - (N-1)/2$. This can be split into three parts:

$$\begin{aligned} f(x,t) \approx \frac{a_{00}}{2} + 2 \cdot \sum_{n=1}^{(N-1)/2} A_{n0} \cos(r_n x + \varphi_{n0}) \\ + 2 \sum_{n=0}^{N-1} \sum_{m=1}^{(M-1)/2} A_{nm} \cos(r_n x + m\omega t + \varphi_{nm}). \end{aligned} \tag{16}$$

Therein, a_{00} corresponds to the DC component and zero order mode of the function f; A_{n0} are all DC components of the space harmonics. The remaining entries, e.g. $A_{nm}\ \forall m = 1 \ldots (M-1)/2,\ n = 0 \ldots N-1$, determine the time and space harmonic waves of f. Therefore, only the latter term of equation (16) is relevant for vibration analysis, as it can represent forward and backward traveling waves. Note that this double sum ranges from 1 to only $(M-1)/2$ which means, that the transformed matrix $\bar{Y}$ only contains half as much entries as Y. However, these entries are complex in contrast to the entries of Y, which have been assumed to be real. Practically, that means only positive frequencies, but positive and negative wave numbers r_n occur.

Of course, the definition could also be chosen to have positive and negative frequencies and only positive wave number. The first convention is used in this paper.

The coefficients in equations (15) and (16) are determined by:

$$a_{nm} = c_{nm} + c_{(N-n)(M-m)}, \tag{17}$$

$$b_{nm} = j(c_{nm} - c_{(N-n)(M-m)}), \tag{18}$$

$$A_{nm} = \sqrt{(a_{nm})^2 + (b_{nm})^2} \text{ and} \tag{19}$$

$$\varphi_{nm} = \arctan\left(\frac{b_{nm}}{a_{nm}}\right). \tag{20}$$

3.2 Concept of space vectors

Space vectors are frequently used as a tool to describe and calculate the flux model of vector controlled electrical machines under various operation modes. However, space vectors offer also a more general description for arbitrary one-dimensional harmonic waves in electrical machines. A graphic definition of space vectors defined as complex numbers was first proposed for electrical machines by Kovács and Štěpina. It allows a handling of harmonic waves in a convenient way (Štěpina, 1989). A single harmonic wave can be expressed by:

$$f(\alpha) = F_p \cdot \cos[p(\alpha - \alpha_0) + \omega(t - t_0)] = F_p \cdot Re\{e^{j(p\alpha_0 + \omega t_0)} e^{-j(p\alpha + \omega t)}\}. \tag{21}$$

The space vector is defined as the complex number:

$$\underline{F} = F_p \cdot e^{j(p\alpha_0 + \omega t_0)}. \tag{22}$$

In this way, the air gap field and magnetic force waves can be described by rotating vectors in the complex plane. The magnitude of the vector corresponds to the wave amplitude, whereas the angle corresponds to the phase shift as shown in Figure 1.

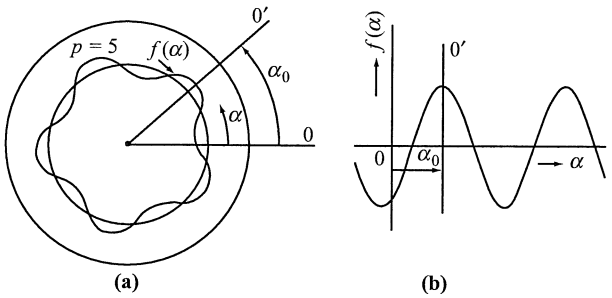

Source: Štěpina (1989)

Figure 1.
General illustrations of one-dimensional harmonic waves: (a) wave with p = 5; (b) value along angle

3.3 Convolution approach

In the sampling procedure in space and time, a full period and a full revolution of the FEM solution data are stored into matrix B. In order to consider the magnetic force density waves, the magnetic force density matrix P is created by applying equation (5) to each matrix entry b_{kl}. Subsequently, a two-dimensional DFT of P provides the approximated Fourier series coefficient $\bar{p}_{nm}$. Path $(B, P, \bar{P})$ in Figure 2 illustrates this approach. The matrix $\bar{P}$ contains space vectors of harmonic magnetic force waves.

Path $(B, \bar{B}, \bar{P})$ in Figure 2 indicates an alternative way of calculating magnetic force density waves $\bar{P}$. First, the 2D DFT is applied directly to the air gap field matrix B. Then, $\bar{P}$ is obtained by matrix convolution. The two-dimensional periodic matrix convolution:

$$Z = X * Y \tag{23}$$

of two given matrices $X, Y \in \mathbb{C}^{K \times L}$ is defined by:

$$z_{s,t} = \sum_{k=1}^{K} \sum_{l=1}^{L} y_{k,l} \cdot y_{s-k,t-l}, \tag{24}$$

It can be shown that a multiplication in time domain, e.g. B^2 corresponds to a convolution in frequency domain, e.g. $\bar{B} * \bar{B}$ (Oppenheim *et al.*, 1999).

Applied to the air gap field DFT matrix, a periodic matrix convolution combines all matrix entries with each other:

$$\bar{P} = \frac{1}{2\mu_0} \cdot \bar{B} * \bar{B}. \tag{25}$$

This approach seems to be complex and costly. A complete convolution (24) for all matrix entries would indeed be very time consuming. However, a complete convolution is not necessary since only a very small number of combination pairs do contribute significantly to the magnetic force density wave that really cause audible noise. Therefore, only the matrix entries of $\bar{b}_{nm}$, whose amplitude exceed a chosen threshold need to be considered in the calculation.

The advantage of this approach in contrast to path $(B, P, \bar{P})$, arises from the fact that each air gap field convolution pair is known and can be stored. Thus, for each resulting force density wave $\bar{p}_{nm}$ a set of pairs:

$$\bar{p}_{nm} : \{(\bar{b}_{n_1 m_1}, \bar{b}_{n_2 m_2}); (\bar{b}_{n_3 m_3}, \bar{b}_{n_4 m_4}); \ldots\} \tag{26}$$

is stored.

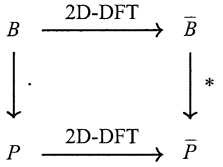

Figure 2.
Commutative diagram

As an example result of such calculation, Table II shows the largest five contributions to the second order, mode two, excitation force density wave. The wave numbers and frequency orders must be added or subtracted to obtain $r = -2$ and $\omega/\omega_0 = 2$ according to equation (8).

3.4 Space vector diagram

Following the convolution approach $(B, \bar{B}, \bar{P})$, each magnetic force wave can be decomposed into the geometric addition of partial space vectors as shown in Figure 3, which represents the same data as Table II. The depicted magnetic force density wave has mode number $r = -2$ and a frequency order of $\omega/\omega_0 = 2$. Each of the partial vectors (*A*), (*B*), (*C*), etc. is associated with an air gap field combination pair. The partial vectors are sorted according to their magnitude. The broken line is the total magnetic force density vector calculated using path $(B, P, \bar{P})$. Obviously, the chain of partial vectors adds up to the total vector. A truncation error that depends on the chosen convolution threshold and on the number of stored partial vectors leads to a gap between the total vector and the vector chain.

Space vector	w/w_0	v	w/w_0	v
A	2	−2	4	−4
B	4	−4	6	−6
C	1	−1	5	−3
D	3	−3	5	−5
E	1	−1	1	−1
	$r = -2$; $w/w_0 = 2$; $p_{tot} = 24,556$ N/m^2 < 115°			

Table II.
Contributing air gap fields

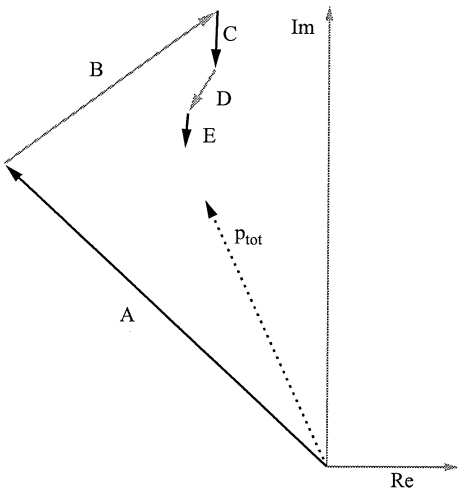

Figure 3.
Space vector diagram for $r = -2$ and $\omega/\omega_0 = 2$

4. Numerical results

4.1 Example machine

To demonstrate the proposed method, a permanent magnet excited synchronous machine (PMSM) is investigated. It is designed using in-house software for the automated sizing of PMSM (Hafner *et al.*, 2008). The machine data are shown in Table III. Its cross-section together with the field distribution in rated operation can be seen from Figure 4. Figure 5 shows the FE mesh, which is used.

The magnetic flux density is sampled in the air gap, this is done for each time step individually. The radial field for one time instance and its spatial spectrum can be seen from Figures 6 and 7, respectively. The spectrum of the resulting force density waves are shown in Figure 8. The convolution of the fundamental field with it self typically yields high amplitudes, in this case it is 162,775 N/m^2. The scale of Figure 8, however, was chosen to clearly depict the most relevant higher force density harmonics of modes $r = 0$, 2 and 4 and only the maximum amplitude of the positive and negative modes is shown.

The convolution approach is applied to the air gap field sampled in time and space. As a first example, the second temporal order, mode 4 force density harmonic, which is supposed to be excited by the fundamental field convoluted by itself, is analyzed. All flux density waves that are larger than 0.01 per cent of the fundamental field are considered as convolution partners. The space vector diagram of Figure 9 shows the three most relevant partial space vectors. Their wave numbers and orders are given in Table IV. The fundamental field squared (*A*) adds by far the largest contribution, however, at least one more flux density wave (*B*) shows a minor influence.

As a second example, the 12th temporal order, mode 0 force density is considered. As shown in Figure 8 this harmonic has a significantly lower amplitude of 1,042 N/m^2, but is still among the most significant higher frequency orders. The space vector diagram of Figure 10 shows a different geometric addition. The force wave is not determined by only one partial vector, but it contains significant at least two equally significant partial vectors (*A*) and (*B*). The wave numbers and frequency orders are given in Table V. A small gap between the total force density vector and the sum of the vectors (*A*) to (*F*) show the asymptotic nature of the proposed method. The wave numbers and frequency orders of the considered force density waves are summarized in Table II. Further application examples of the proposed method can be found in (van der Giet *et al.*, 2008).

Table III.
Machine data of the example PMSM

Machine data	Value
Number of pole pairs (p)	2
Rated power (P_n)	2 kW
Rated speed (n_n)	4,500 rpm
Rated voltage (V_n)	230 V
Rated current (I_n)	11.2 A
Outer stator diameter (D_o)	110 mm
Inner stator diameter (D_i)	60 mm
Mechanical air gap (δ)	0.8 mm
Active length (l_{Fe})	120 mm
Number of stator slots (N_1)	24

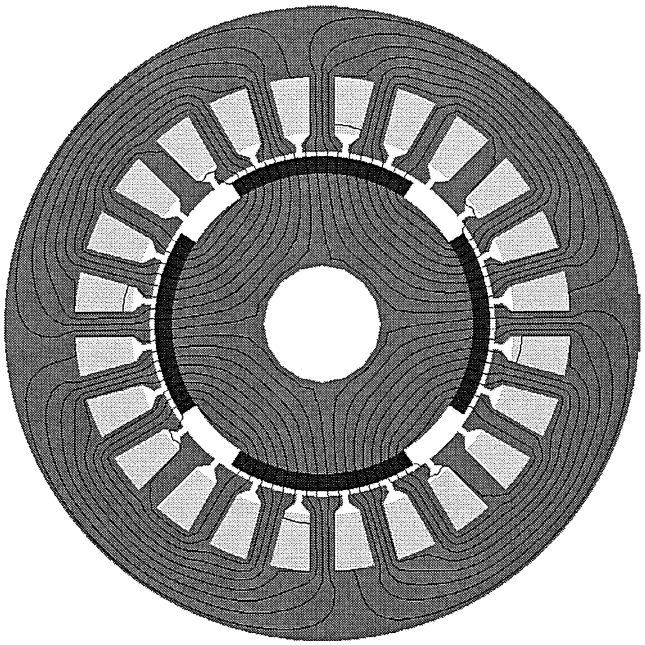

Figure 4.
Stator and rotor of four pole example PMSM with field lines

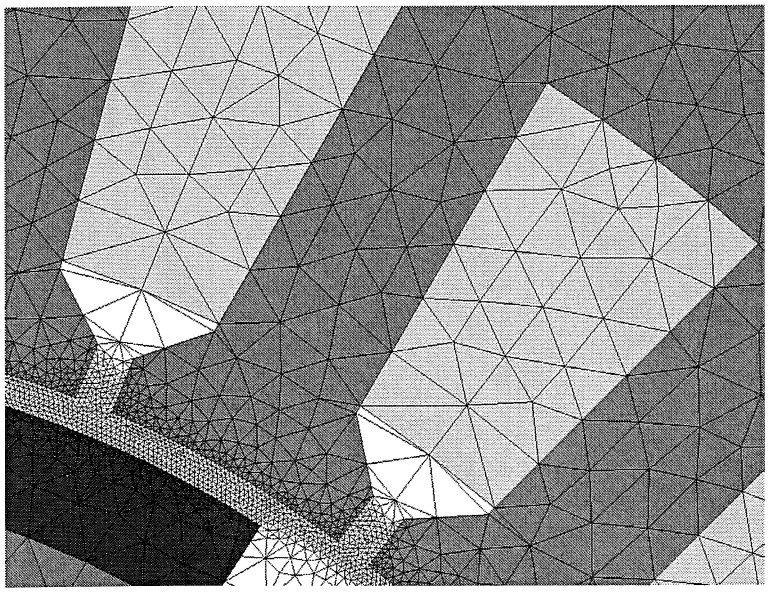

Figure 5.
FE mesh

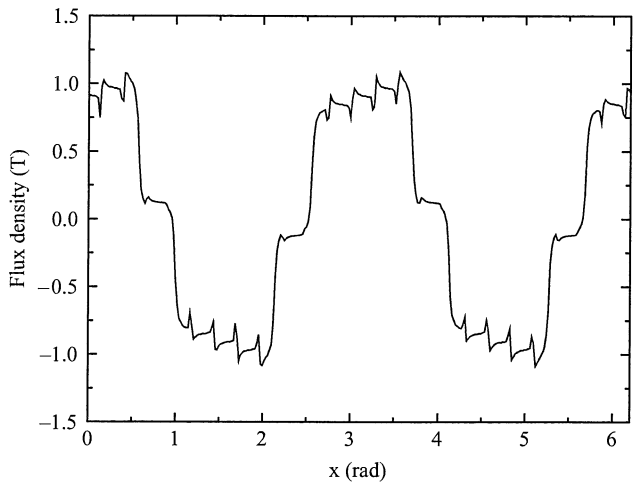

Figure 6.
Radial air gap flux density

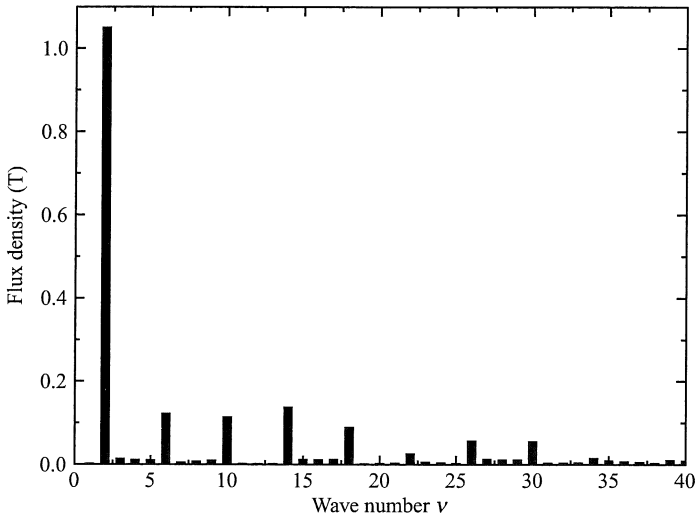

Figure 7.
Radial air gap flux density spectrum

4.2 Comparison with full stress tensor calculation

To justify the approach and to investigate its limits, the force density in mode-frequency domain obtained from stress tensor using equation (1), which would be typically used for a subsequent structural dynamic simulation, is compared to the simplified formula (5). Figure 11 shows the relative deviation between those two. For the fundamental field square, its magnitude is used as reference value, for all other waves, 2,000 N/m^2 is used as reference value, which corresponds to the maximum amplitude shown in Figure 8. The deviation of the angle between the calculation using equations (1) and (5) is shown in Figure 12 for all waves with an amplitude larger than 600 N/m^2, which is less than 0.5 per cent of the amplitude of the fundamental field squared. It can be seen that the relative error is below 40 per cent and the angle error is

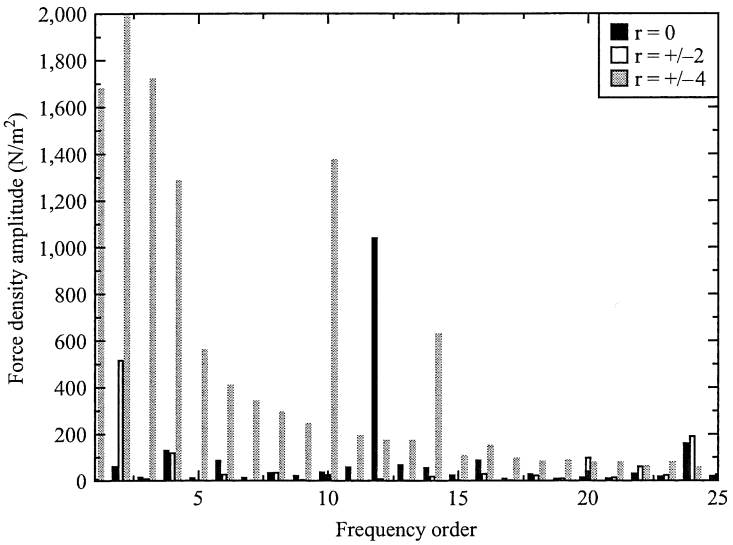

Figure 8.
Force density amplitude of different modes

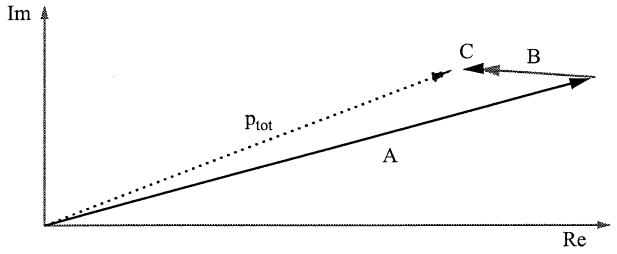

Figure 9.
Space vector diagram for $r = -4$ and $\omega/\omega_0 = 2$

Space vector	w/w_0	v	w/w_0	v
A	1	−2	1	−2
B	1	−2	3	−6
C	5	−10	7	−14
	$r = -4$; $w/w_0 = 2$; $p_{tot} = 170{,}258\,\mathrm{N/m^2} < 20°$			

Table IV.
Contributing air gap fields

less than 30° for all shown harmonics. The deviation is still significant as to use the full stress tensor calculation for the excitation of precise structural dynamic simulations, however, the obtained accuracy can be considered sufficient for studying the contributions of the individual flux density waves to a particular force wave.

5. Summary and conclusions

The method presented in this paper allows the determination of the contributions of partial force density waves to a specific force density waves. The approach is based on the 2D Fourier transform representation of the magnetic flux density in the air gap and

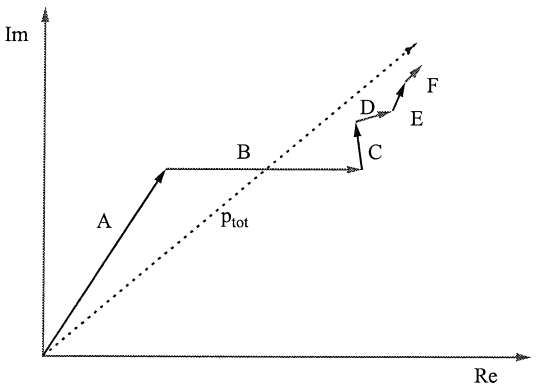

Figure 10.
Space vector diagram for $r = 0$ and $\omega/\omega_0 = 12$

Space vector	w/w_0	v	w/w_0	v
A	1	−26	13	−26
B	1	−2	11	2
C	1	−2	13	−2
D	5	14	7	−14
E	3	18	9	−18
F	3	−30	15	−30
	$r = 0$; $w/w_0 = 12$; $p_{tot} = 1,042\,\mathrm{N/m^2} < 40°$			

Table V.
Contributing air gap fields

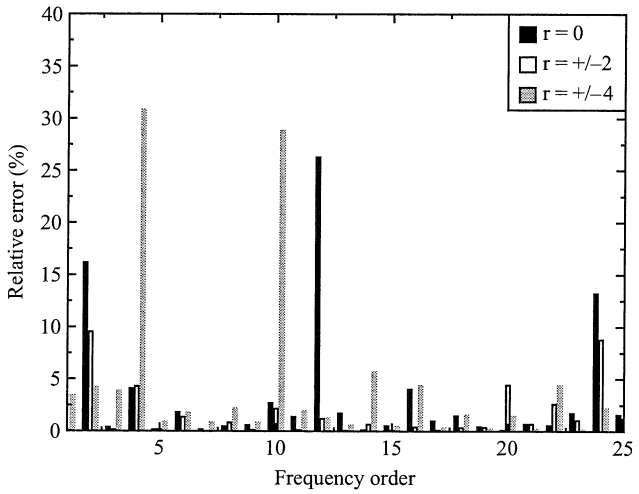

Figure 11.
Deviation between MST and $B^2/2\mu_0$

its convolution with itself. It is shown that the convolution can be limited to the computation of the most relevant matrix entries. As an example, the air gap field and the force density waves of a PMSM are analyzed to demonstrate the effectiveness of the proposed approach. For this example, the error between the full stress tensor

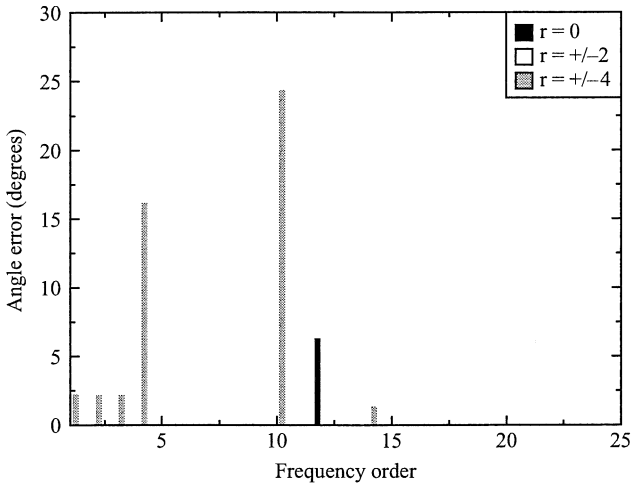

Figure 12.
Deviation between MST and $B^2/2\mu_0$

calculation and its simplified version is analyzed. The error is not negligible, but is still small enough to apply the proposed approach in noise and vibration diagnosis of electrical machine.

References

Furlan, M., Cernigoj, A. and Boltezar, M. (2003), "A coupled electromagnetic-mechanical-acoustic model of a dc electric motor", *COMPEL: The International Journal for Computation and Mathematics in Electrical and Electronic Engineering*, Vol. 22 No. 4, pp. 1155-65.

Gieras, J., Wang, C. and Lai, J.C. (2006), *Noise of Polyphase Electric Motors*, CRC Press, Boca Raton, FL.

Hafner, M., Schöning, M. and Hameyer, K. (2008), "Automated sizing of permanent magnet synchronous machines with respect to electromagnetic and thermal aspects", *Proceedings of the 2008 International Conference on Electrical Machines, Vilamoura, Portugal.*

Henrotte, F. and Hameyer, K. (2007), "A theory for electromagnetic force formulas in continuous media", *IEEE Transactions on Magnetics*, Vol. 43 No. 4, pp. 1445-8.

Jordan, H. (1950), *Geräuscharme Elektromotoren*, W. Girardet, Essen.

Kobayashi, T., Tajima, F., Ito, M. and Shibukawa, S. (1997), "Effects of slot combination on acoustic noise from induction motors", *IEEE Transactions on Magnetics*, Vol. 33 No. 2, pp. 2101-4.

Melcher, J. (1981), *Continuum Electromechanics*, MIT Press, Cambridge, MA.

Oppenheim, A., Schafer, R. and Buck, J. (1999), *Discrete-Time Signal Processing*, 2nd ed., Prentice-Hall, Englewood Cliffs, NJ.

Schlensok, C., Schmülling, B., van der Giet, M. and Hameyer, K. (2007), "Electromagnetically excited audible noise evaluation and optimization of electrical machines by numerical simulation", *COMPEL: The International Journal for Computation and Mathematics in Electrical and Electronic Engineering*, Vol. 26, pp. 727-42.

Štěpina, J. (1989), "Komplexe Größen in der Elektrotechnik", *Archiv für Elektrotechnik (Electrical Engineering)*, Vol. 72 No. 6, pp. 407-14.

van der Giet, M., Rothe, R., Herranz Gracia, M. and Hameyer, K. (2008), "Analysis of noise exciting magnetic force waves by means of numerical simulation and a space vector definition", *Proceedings of the 2008 International Conference on Electrical Machines, Vilamoura, Portugal.*

About the authors

M. van der Giet received his Dipl.-Ing. degree in electrical engineering in 2004 as Engineer from the Faculty of Electrical Engineering and Information Technology at the RWTH Aachen University. Since 2004, he has worked as a researcher at the Institute of Electrical Machines (IEM) at the RWTH Aachen University. He is currently working towards his PhD degree in the area of noise and vibration of electrical machines. M. van der Giet is the corresponding author and can be contacted at: Michael.vanderGiet@IEM.RWTH-Aachen.de

R. Rothe received his Dipl.-Ing. degree in electrical engineering in 2007 as Engineer from the Faculty of Electrical Engineering and Information Technology at the RWTH Aachen University. Since 2007, he has worked as a researcher at the IEM at the RWTH Aachen University. He is currently working towards his PhD degree and his current research interests are the numerical field simulation of electro-magnetic devices.

K. Hameyer received the Dipl.-Ing. degree in electrical engineering from the University of Hannover, Germany. He received the PhD degree from University of Technology Berlin, Germany. After his university studies he worked with the Robert Bosch GmbH in Stuttgart, Germany, as a Design Engineer for permanent magnet servo motors and board net components. In 1988, he became a member of the staff at the University of Technology, Berlin, Germany. Until February 2004 Dr Hameyer was a full Professor for Numerical Field Computations and Electrical Machines with the KU Leuven in Belgium. Currently, Dr Hameyer is the head of the IEM, holder of the chair "Electromagnetic Energy Conversion" and Dean of the Faculty of Electrical Engineering and Information Technology at the RWTH Aachen University in Germany. His research interests are numerical field computation, the design of electrical machines, in particular permanent magnet excited machines, induction machines and numerical optimization strategies.